On the simultaneous description of H-bonding and dipolar interactions with point charges in force field models

Kai Langenbach*, Cemal Engin, Steffen Reiser, Martin Horsch, Hans Hasse

Laboratory of Engineering Thermodynamics, University of Kaiserslautern,
Erwin-Schrödinger-Strasse, 67663 Kaiserslautern, Germany

Abstract

H-bonding and polar interactions occur together in real fluids, but are of different nature and have different effects on macroscopic properties. Nevertheless, both are usually described by point charges in force field models. We show that, despite this, the two effects can be separated. We study a simple model fluid: a single Lennard-Jones site with two opposing point charges q placed in the center of the Lennard-Jones site and at a distance d. By suitably varying both d and q the dipole moment μ is kept constant. Both μ and d are systematically varied to study the properties of the resulting models, including H-bonding, which is determined using a geometric criterion from literature. We show that d can be used for tuning the H-bonding strength and, thus, polarity and H-bonding can be adjusted individually. The study of a second related model with symmetrically positioned point charges does not reveal this separation.

Keywords:

hydrogen bonding, polarity, point charge, molecular modeling, force fields, thermodynamics

Highlights:

- A new type of simple force field is introduced: the beak model.
- The beak model is the simplest model, which accounts for repulsion, dispersion, polarity, and hydrogen bonding.
- Beak type groups are common in molecular modeling of polar hydrogen bonding fluids.

* Author to whom correspondence should be addressed.
Tel.: +49 631 205 2176
Fax: +49 631 205 3835
Email: Kai.Langenbach@mv.uni-kl.de

- The study illustrates how the separation between polarity and hydrogen bonding is achieved in beak type models.
- The results can be used for developing equations of state.

Introduction

H-bonding has been in the focus of research for many decades, but there is still no unambiguous definition of what an H-bond is. It is common practice to consider a molecular interaction between different sites as an H-bond if the following criteria are met[1]:

- It is a highly directional and short-ranged.
- It has stoichiometric properties, meaning that there is always a donor and an acceptor and there may not be an arbitrary number of bonds involving one particular site.

Several criteria have been proposed in the literature to distinguish between bonded and non-bonded sites[2–8], some of which are of geometrical nature[5–8], while others are energetic rules[6].

There are two common ways for describing H-bonds by force fields. In the first, short-ranged potentials, the so-called bonding sites are introduced for describing H-bonding. In the well-known approach of Wertheim[9], a square-well potential is used for this. In the second, appropriately placed point charges are used for describing H-bonding. It has been shown previously that the above mentioned criteria of H-bonding can be met with this electrostatic approach[10]. Furthermore, it has been shown that also structural properties of H-bonding fluids such as radial pair distribution functions can be described well with that model class[10,11]. The present work contributes to elucidating how that electrostatic approach for modeling H-bonding works and, namely, how H-bonding and polarity can be separated using that approach.

The electrostatic approach is very common for describing H-bonding polar fluids with force fields. Examples are the models of Schnabel *et al.*[10,12–14], as well as others[11,15], to name only a few. In these models, the H-bonding groups in the molecules are usually described by Lennard-Jones (LJ) sites with point charges, one of which is typically placed in the center of the LJ site. Such arrangements of the charges on the core structure resemble a beak, cf. Figure 1. Hence, this model type is called “beak model” here, the corresponding fluid is called beak fluid.

Using such beak groups with partial charges for modeling H-bonding poses a fundamental problem: can polarity and H-bonding be described independently with such models? That question is addressed here by systematically studying a very simple model fluid which consists only of the beak group. We call this the beak model henceforth. It is a single LJ site with a partial charge q in its center and a second partial charge $-q$ at a certain distance d. By suitably varying both d and q the dipole moment μ can be kept constant. Here the beak model is specified by giving μ and d which are systematically varied in our study. Note that throughout the present work, dimensionless properties are used as defined in Appendix A. For different combinations of μ and d the vapor-liquid equilibrium of the beak model is studied. Finally, for corresponding liquid states the H-bonding is quantified using a geometric criterion from literature[7]. The results show that by adjusting the distance d the strength of the H-bonding in the fluid can be varied at constant μ.

Besides the beak group, a second closely related model is studied in which both charges are arranged symmetrically on the LJ site. It is shown that this model, despite its close relationship to the beak model, does not enable the desired separation of hydrogen bonding and polarity.

Molecular Model

In this study two types of molecular models are studied, *cf.* Figure 2. The first is the beak model (*cf.* Figure 2, left). It consists of a single LJ site with two point charges q and $-q$, one of which is placed in the LJ center, while the other one is placed at a distance $d \leq 0.5$ from the center. Table 1 gives an overview of the studied parameter combinations, which cover the range typically encountered in beak type groups in the literature.

The second model, which is called “symmetric model” here, is a modification of the Stockmayer potential, in which instead of a point dipole two symmetrically arranged point charges (q and $-q$ at a distance d) are used (*cf.* Figure 2, right). The parameter combinations, for which the symmetric model was studied, are the same as those for the beak model, *cf.* Table 1.

Hydrogen Bonding Criteria

Form the large number of H-bonding criteria which are described in the literature, we have chosen for the present study the geometric criterion of Haughney *et al.*[7]. This choice follows previous work of our group[10,11,14]. Kumar *et al.*[6] have compared different H-bonding

criteria for liquid water and have found only little influence on the calculated total number of H-bonds, although the results for the distribution of the H-bonded species varied. Using the criterion of Haughney *et al.*[7], the fractions f_i of molecules with i = 0, 1, 2, and 3 hydrogen bonds per molecule were evaluated. Hence, f_0 counts monomers, f_1 counts molecules at ends of H-bonded chains including dimers, f_2 counts molecules in chains which are not at ends, and f_3 counts molecules at which branching of chains occurs.

Simulations

The vapor-liquid equilibrium (VLE) of the beak model and the symmetric model is calculated using the Grand Equilibrium (GE) method[16] for the parameter combinations specified in Table 1. Details on the simulations are given in Appendix B. The temperature is varied between about 0.8 and 0.95 of the critical temperature of the studied fluid. Following previous work of our group[17] Guggenheim-type expressions are fitted to the simulation data to calculate the critical points. If the resulting critical temperatures reveal that temperatures below 0.8 of the critical temperature were used in the process, the fit is repeated excluding this data. Once the critical point of each model is known, MD simulations at 0.7 of the critical temperature are carried out in which the H-bonding statistics are evaluated. For convenience, the pressure was kept constant in these liquid phase simulations and set to p = 0.015. The deviations between these results and results which would be obtained for the boiling point pressure at the same temperature are not important here so that we argue that the comparison of the different models is carried out for corresponding states.

Results and Discussion

Numerical results of the simulations are given in Appendix C.

The results of the VLE study of the beak model are shown in Figure 4 to Figure 6. Figure 4 shows the saturated densities for different combinations of μ and d. Both parameters have a significant influence on the shape and location of the binodal. As expected, at constant d an increase of μ leads to an increase of the critical temperature. But also an increase of d at constant μ leads to an increase of the critical temperature (*cf.* Figure 3). The same critical point can be achieved for a smaller μ, if d is simultaneously increased. For higher values of μ, the influence of d on the critical temperature increases.

The critical temperatures of the studied beak fluids are depicted in Figure 3. The critical temperature depends systematically on both μ and *d*. The critical temperature of the Stockmayer fluid[18], which is the limiting case of the beak fluid for $d \to 0$, is included for comparison. The critical pressure was determined from the critical temperature and an Antoine fit of the vapor pressure data (see next paragraph) in the same range of temperatures used to calculate the critical temperature. The critical pressure neither depends significantly on μ nor on *d*. The number found for the critical pressure is around 0.14. This is in agreement with previous findings for the Stockmayer fluid[18] for dipole moments in the range which was studied here. There, numbers for the critical pressure of 0.13-0.14 are reported. The corresponding number for the LJ fluid is 0.13[17] which underlines that the finding of a constant critical pressure holds only in the studied parameter range.

Figure 5 shows the vapor pressure curves of the studied beak fluids. Although the critical pressure is influenced neither by μ nor by *d* the slope of the vapor pressure curve is. It decreases with both parameters increasing. Figure 6 shows the enthalpy of vaporization against temperature for the same models. This quantity increases with both μ and *d*, where μ has the stronger influence. For large numbers of μ also the sensitivity to *d* increases.

Using the information on the critical points, it is possible to calculate the acentric factor ω from the vapor pressure curve. The acentric factor ω is plotted in Figure 7 against μ^2 for two different numbers of *d*. It increases both with increasing μ and *d*.

Together, Figure 3-7 show that the macroscopic properties of the beak fluid depend both on μ and *d*. Namely, for the same dipole moment μ, different numbers for *d* result in significantly different thermodynamic behavior. The trends which are observed at constant μ for increasing numbers of *d* are those that would be expected for increasingly attractive interactions. It is shown now that they can be interpreted as resulting from an increase in H-bonding strength.

The studies of H-bonding statistics are carried out for corresponding liquid states at temperatures of 0.7 of the critical temperature as discussed above. For three different numbers of μ the influence of *d* on the H-bonding statistics is studied. The results are presented in Figure 8, where the fractions f_i of molecules with *i* = 0, 1 and 2 hydrogen bonds are shown from top to bottom. The fraction f_3 is omitted, as the numbers are small (*cf.* numerical data in Appendix C). The influence of *d* matches the expectations for a property describing the hydrogen bonding strength: with increasing numbers of *d* the monomer fraction decreases significantly. At low numbers of *d*, *i.e.* for fluids, which are similar to the Stockmayer fluid

practically no association is observed and the molecules are only present as monomers. On the other hand, for large numbers of *d* the H-bonding gets so strong that hardly any monomers are found. There is a certain influence of the dipole moment μ on all this, where large numbers of μ lead to an increase in the H-bonding. Hence, polarity and H-bonding are not completely separated in the beak model. But at constant μ an increase of *d* leads to increased H-bonding strength. The findings for f_1 and f_2 fit into this picture. The fraction f_1 of molecules with one hydrogen bond, *i.e.* end groups in chains has a maximum when plotted over *d*. With increasing H-bonding strength (increasing *d*), first f_1 increases as dimers form but then, as the chains become longer f_1 decreases again. The growing chain length also results in in an increase of f_2. As for f_0 there is also an influence of μ on f_1 and f_2. Again, large numbers of μ lead to an increase in the H-bonding.

The low numbers of f_3 show that the associates are not branched. In principle, they could be either linear or cyclic. Cyclic associates are not readily identified, but a visual inspection of the simulation results indicates that there are no substantial amounts of cyclic associates present in the beak fluid.

The VLE calculated for the symmetric model is depicted in Figure 9. The studied combinations of μ and *d* are the same as for the beak model, so that the results can be compared directly to those shown in Figure 4. As *d* goes to zero both the symmetric model and the beak model approach the Stockmayer model. As for the beak model, also for the symmetric model, a strong influence of μ on the thermodynamic properties is observed. However, the influence of *d* on the thermodynamic properties of the symmetric model is small. The symmetric model can be considered as a discretized version of the Stockmayer fluid for which at large numbers of *d* some deviations occur. That influence of *d* on the thermodynamic properties is only discernible at large numbers of μ and should not be attributed to H-bonding. Therefore, the symmetric model is not further investigated here.

Conclusions

In this paper, a simple model fluid was studied: the beak fluid. It is described by the beak model which is closely related to the Stockmayer model. However, the dipole is represented by two point charges in the beak model, one of which on is in the center of the Lennard-Jones site. That model can be described by two dimensionless parameters for which we choose the dipole moment μ and the distance of the charges *d*. These two parameters are

varied systematically over a significant range and vapor-liquid equilibria over a wide range of temperatures are calculated for each combination of the parameters. From that data, the critical points are calculated by fitting Guggenheim type expressions. The vapor-liquid equilibrium as well as the critical point depend significantly on both μ and d. The results show that increasing d leads to increasingly attractive interactions. In a further step, H-bonding in the beak fluid is studied for corresponding liquid states for all parameter combinations. The results reveal that d can be used to tune the strength of the H-bonding in the fluid. Also the choice of μ has an influence on H-bonding, but at constant μ the parameter d enables adjusting the strength of the H-bonding.

The beak model is only the simplest representative of a widely used class of force fields that are used for describing polar and H-bonding fluids. These models contain groups which are similar to the beak model for representing H-bonding groups in the real fluid (beak groups). The results from the present study illustrate how the separation of polarity and H-bonding in beak type models is achieved: Polarity and H-bonding can be adjusted individually and the strength of the H-bonding is adjusted by choosing d. As beak groups are widely used in molecular modeling, this is of broad interest. The results can also be used for developing molecular equations of state which account for both polarity and H-bonding.

Besides the beak model, a second closely related model is studied, in which both charges are arranged symmetrically around the center of the Lennard-Jones site. It is shown that this model, despite its close relationship to the beak model, behaves quite differently and shows only little influence of d on the thermodynamic properties.

Acknowledgements

The authors would like to thank Richard H. Henchman for fruitful discussions and Alptekin Celik for performing parts of the simulations. Funding by the German Federal Ministry of Education and Research (BMBF) for the SkaSim project and Deutsche Forschungsgemeinschaft's (DFG) Reinhart Koselleck program is gratefully acknowledged. The presented research was conducted under the auspices of the Boltzmann-Zuse Society of Computational Molecular Engineering (BZS), and the simulations were performed on the *elwetritsch* cluster, Regionales Hochschulrechenzentrum Kaiserslautern, within the scientific computing project TUKL-MSWS.

References

1. Arunan E, Desiraju GR, Klein RA, et al. Defining the hydrogen bond: An account (IUPAC Technical Report). *Pure Appl. Chem.* 2011;83(8):1619-1636.
2. Jorgensen WL. Monte Carlo results for hydrogen bond distributions in liquid water. *Chem. Phys. Lett.* 1980;70(2):326-329.
3. Rapaport DC. Hydrogen bonds in water. *Mol. Phys.* 1983;50(5):1151-1162.
4. Matsumoto M, Ohmine I. A new approach to the dynamics of hydrogen bond network in liquid water. *J. Chem. Phys.* 1996;104(7):2705.
5. Starr FW, Nielsen JK, Stanley HE. Hydrogen-bond dynamics for the extended simple point-charge model of water. *Phys. Rev. E* 2000;62(1):579-587.
6. Kumar R, Schmidt JR, Skinner JL. Hydrogen bonding definitions and dynamics in liquid water. *J. Chem. Phys.* 2007;126(20):204107-204107-12.
7. Haughney M, Ferrario M, McDonald IR. Molecular-dynamics simulation of liquid methanol. *J. Phys. Chem.* 1987;91(19):4934-4940.
8. Hammerich AD, Buch V. An alternative near-neighbor definition of hydrogen bonding in water. *J. Chem. Phys.* 2008;128(11):111101.
9. Wertheim MS. Fluids with highly directional attractive forces. I. Statistical thermodynamics. *J. Stat. Phys.* 1984;35:19-34.
10. Schnabel T, Srivastava A, Vrabec J, Hasse H. Hydrogen Bonding of Methanol in Supercritical CO2: Comparison between 1H NMR Spectroscopic Data and Molecular Simulation Results. *J. Phys. Chem. B* 2007;111(33):9871-9878.
11. Reiser S, McCann N, Horsch M, Hasse H. Hydrogen bonding of ethanol in supercritical mixtures with CO2 by 1H NMR spectroscopy and molecular simulation. *J. Supercrit. Fluids* 2012;68:94-103.
12. Schnabel T, Vrabec J, Hasse H. Henry's law constants of methane, nitrogen, oxygen and carbon dioxide in ethanol from 273 to 498 K: Prediction from molecular simulation. *Fluid Phase Equilibria* 2005;233(2):134-143.
13. Schnabel T, Cortada M, Vrabec J, Lago S, Hasse H. Molecular model for formic acid adjusted to vapor–liquid equilibria. *Chem. Phys. Lett.* 2007;435(4–6):268-272.
14. Schnabel T, Vrabec J, Hasse H. Molecular simulation study of hydrogen bonding mixtures and new molecular models for mono- and dimethylamine. *Fluid Phase Equilibria* 2008;263(2):144-159.
15. Van Leeuwen ME, Smit B. Molecular Simulation of the Vapor-Liquid Coexistence Curve of Methanol. *J. Phys. Chem.* 1995;99(7):1831-1833.
16. Vrabec J, Hasse H. Grand Equilibrium: vapour-liquid equilibria by a new molecular simulation method. *Mol. Phys.* 2002;100(21):3375-3383.
17. Lotfi A, Vrabec J, Fischer J. Vapour liquid equilibria of the Lennard-Jones fluid from the NpT plus test particle method. *Mol. Phys.* 1992;76(6):1319-1333.
18. Van Leeuwen ME. Deviation from corresponding-states behaviour for polar fluids. *Mol. Phys.* 1994;82(2):383-392.
19. Deublein S, Eckl B, Stoll J, et al. ms2: A molecular simulation tool for thermodynamic properties. *Comput. Phys. Commun.* 2011;182(11):2350-2367.
20. Nezbeda I, Kolafa J. A New Version of the Insertion Particle Method for Determining the Chemical Potential by Monte Carlo Simulation. *Mol. Simul.* 1991;5(6):391-403.
21. Lyubartsev AP, Martsinovski AA, Shevkunov SV, Vorontsov-Velyaminov PN. New approach to Monte Carlo calculation of the free energy: Method of expanded ensembles. *J. Chem. Phys.* 1992;96(3):1776-1783.
22. Lyubartsev AP, Laaksonen A, Vorontsov-Velyaminov PN. Free energy calculations for Lennard-Jones systems and water using the expanded ensemble method: A Monte Carlo and molecular dynamics simulation study. *Mol. Phys.* 1994;82(3):455-471.
23. Vrabec J, Kettler M, Hasse H. Chemical potential of quadrupolar two-centre Lennard-Jones fluids by gradual insertion. *Chem. Phys. Lett.* 2002;356(5–6):431-436.

24. Nymand TM, Linse P. Ewald summation and reaction field methods for potentials with atomic charges, dipoles, and polarizabilities. *J. Chem. Phys.* 2000;112(14):6152-6160.
25. Frenkel D, Smit B. *Understanding Molecular Simulation from Algorithms to Applications*. San Diego: Academic Press; 2002.

Appendix A. Reduced units

The reduced properties used in this article are the reduced separation of the partial charges

$$d^* = \frac{d}{\sigma} \tag{A.1}$$

in units of the LJ diameter σ, the reduced temperature

$$T^* = \frac{T}{k_B \varepsilon} \tag{A.2}$$

in units of the Boltzmann constant k_B and the LJ interaction energy ε, the reduced dipole strength

$$\mu^{*2} = \frac{\mu^2}{4\pi\varepsilon_0 \varepsilon \sigma^3}, \tag{A.3}$$

where ε_0 is the electrical permittivity of vacuum and the dipole moment μ is linked to the partial charges via

$$\mu = dq, \tag{A.4}$$

the reduced pressure

$$p^{s*} = \frac{p^s \sigma^3}{\varepsilon}, \tag{A.5}$$

reduced density

$$\rho^* = \rho\sigma^3, \tag{A.6}$$

and reduced enthalpy

$$h^* = \frac{h}{\varepsilon}. \tag{A.7}$$

The asterisks are dropped throughout the article for better readability.

Appendix B. Simulation details

All calculations were performed with *ms2*[19] using the GE method[16] in conjunction with MC methods for the coexisting curve and using MD simulations in the *NPT* ensemble for hydrogen bonding statistics. For the MC liquid runs, the equilibration was performed using 10000 *NVT* cycles and 25000 *NPT* cycles, while the production was performed using 50000 cycles in the *NPT* ensemble. In every cycle, 100 displacement moves, 1000 rotation moves and 1 volume move were performed. The gradual insertion technique[20–23] was used to calculate the chemical potential using 10000 fluctuating state change moves, 10000 fluctuating particle moves and 50 000 biased particle translation/rotation moves every 50 cycles. The following vapor runs used 10000 *NVT* steps, 50000 steps in the pseudo μVT ensemble for equilibration and 200000 steps for production. The MD simulations for hydrogen bonding statistics where performed in the *NPT* ensemble with an initial 20000 steps in the *NVT* ensemble followed by 50000 *NPT* steps for equilibration and 200000 run steps. A cut off radius of r_C = 4.5 σ was employed in all simulations and the reaction field method[19,24,25] was used for long range corrections. The initial number of particles in all simulations was chosen as 864.

Appendix C. Simulation results

The current investigation concerning the beak model is divided into three distinct parts, which are the VLE simulation, the critical point determination and the corresponding states analysis of H-bonding. The VLE results are presented in Table 2 for the parameter combinations listed in Table 1. The critical temperatures are shown in Table 3 and the H-bonding results are depicted in Table 4.

Table 1: Combinations of dipole moments μ and point charge distance d used in the simulations of both the beak model and the symmetric model, with symbols as used in Figure 4 to Figure 6 and Figure 9.

d \ μ	1.6	1.8	2	2.2	2.45
0.3	■	□	⊞	⬒	◨
0.4	●	○	⊕	◓	◑
0.5	▲	△	⟁	◬	◭

Table 2: Vapor-liquid equilibrium together with statistical uncertainties of different beak fluids: thermodynamic properties in the saturated states. Statistical uncertainties are indicated with a δ.

T	p_s	$\delta p_s 10^4$	ρ'	$10^3\delta\rho'$	ρ''	$10^4\delta\rho''$	Δh_V	$100\delta\Delta h_V$
			$\mu = 1.6$		$d = 0.3$			
1.200	0.009	0.176	0.795	0.093	0.008	0.163	9.736	0.110
1.300	0.017	0.352	0.754	0.120	0.015	0.309	9.080	0.160
1.400	0.030	0.352	0.710	0.145	0.026	0.309	8.304	0.200
1.410	0.031	0.371	0.706	0.141	0.028	0.341	8.213	0.220
1.515	0.052	2.884	0.651	0.727	0.047	2.650	7.194	1.060
1.590	0.072	3.441	0.606	1.203	0.070	3.317	6.283	1.740
1.640	0.088	4.311	0.571	1.564	0.091	4.423	5.519	2.250
1.690	0.110	4.301	0.534	1.737	0.128	5.008	4.485	2.930
			$\mu = 1.6$		$d = 0.4$			
1.250	0.011	1.075	0.785	0.377	0.010	0.976	9.718	0.420
1.300	0.014	1.329	0.766	0.525	0.013	1.171	9.404	0.620
1.400	0.026	1.662	0.723	0.567	0.023	1.463	8.634	0.710
1.500	0.043	2.776	0.676	0.836	0.039	2.488	7.743	1.010
1.575	0.061	2.786	0.635	1.019	0.056	2.585	6.915	1.380
1.613	0.071	3.421	0.612	1.341	0.068	3.268	6.439	1.840
1.650	0.084	4.369	0.590	2.241	0.084	4.390	5.876	2.590
1.675	0.092	3.646	0.569	1.506	0.095	3.772	5.474	2.490
1.715	0.107	4.360	0.531	3.312	0.118	4.813	4.697	3.270
			$\mu = 1.6$		$d = 0.5$			
1.275	0.010	0.205	0.787	0.101	0.009	0.179	10.001	0.130
1.350	0.016	1.339	0.759	0.454	0.014	1.171	9.487	0.600
1.400	0.022	1.574	0.739	0.631	0.019	1.366	9.110	0.750
1.450	0.028	1.525	0.717	0.558	0.024	1.317	8.708	0.780
1.470	0.031	0.371	0.707	0.141	0.027	0.325	8.534	0.220
1.500	0.036	2.317	0.694	0.693	0.032	2.032	8.250	0.930
1.550	0.045	2.972	0.669	0.751	0.040	2.618	7.779	1.140
1.600	0.058	2.669	0.646	1.013	0.053	2.439	7.216	1.450
1.650	0.071	3.548	0.613	1.042	0.067	3.349	6.583	1.860
1.700	0.085	4.350	0.582	1.605	0.084	4.309	5.900	2.700
1.740	0.102	4.027	0.553	1.849	0.109	4.325	5.112	2.960
1.770	0.114	5.210	0.527	2.002	0.132	6.081	4.444	4.290
			$\mu = 1.8$		$d = 0.3$			
1.350	0.010	0.837	0.784	0.529	0.009	0.701	10.683	0.640
1.450	0.018	1.332	0.745	0.490	0.015	1.098	9.973	0.689
1.550	0.031	1.962	0.702	0.622	0.026	1.628	9.121	0.865
1.650	0.050	2.781	0.657	0.823	0.044	2.413	8.059	1.252

T	p_s	$\delta p_s 10^4$	ρ'	$10^3\delta\rho'$	ρ''	$10^4\delta\rho''$	Δh_V	$100\delta\Delta h_V$
1.700	0.061	3.423	0.628	1.219	0.054	3.029	7.480	1.615
1.750	0.075	3.670	0.595	1.386	0.068	3.371	6.787	2.154
1.800	0.092	3.845	0.565	1.449	0.091	3.816	5.940	2.717
1.800	0.090	4.514	0.558	1.923	0.087	4.372	5.982	2.991
1.850	0.109	4.342	0.523	2.799	0.116	4.626	5.005	4.228
			$\mu = 1.8$		$d = 0.4$			
1.350	0.008	0.760	0.794	0.345	0.007	0.631	11.088	0.526
1.450	0.015	1.270	0.758	0.577	0.013	1.034	10.397	0.751
1.550	0.027	1.682	0.718	0.584	0.022	1.374	9.566	0.875
1.650	0.042	2.376	0.673	0.704	0.035	1.980	8.623	1.133
1.750	0.065	3.010	0.620	1.159	0.058	2.668	7.400	1.778
1.800	0.079	3.183	0.586	1.403	0.073	2.941	6.679	2.182
1.850	0.096	4.100	0.554	1.499	0.096	4.105	5.793	3.095
1.900	0.116	4.983	0.515	2.725	0.135	5.777	4.566	5.470
			$\mu = 1.8$		$d = 0.5$			
1.450	0.012	0.850	0.772	0.459	0.010	0.686	11.019	0.641
1.500	0.016	1.151	0.753	0.633	0.013	0.924	10.631	0.834
1.575	0.024	1.747	0.725	0.679	0.019	1.403	10.022	0.993
1.625	0.030	1.616	0.701	0.745	0.024	1.304	9.542	1.029
1.700	0.042	2.365	0.670	0.800	0.035	1.959	8.783	1.346
1.750	0.053	3.021	0.647	0.876	0.045	2.574	8.202	1.478
1.800	0.064	3.726	0.618	1.126	0.056	3.265	7.572	1.975
1.850	0.079	3.049	0.590	1.504	0.074	2.844	6.780	2.489
1.900	0.094	3.890	0.553	1.861	0.093	3.850	5.946	2.947
1.950	0.111	4.863	0.507	2.996	0.118	5.182	4.927	4.578
			$\mu = 2$		$d = 0.3$			
1.450	0.008	0.692	0.796	0.454	0.006	0.537	12.251	0.684
1.550	0.014	0.987	0.760	0.642	0.010	0.751	11.529	0.894
1.650	0.023	1.462	0.724	0.644	0.018	1.119	10.697	0.941
1.750	0.036	1.978	0.680	0.674	0.028	1.535	9.738	1.064
1.850	0.056	3.198	0.634	0.989	0.046	2.629	8.540	1.855
1.900	0.068	3.573	0.605	1.320	0.058	3.067	7.820	2.732
1.950	0.081	4.249	0.578	1.286	0.073	3.813	7.095	2.974
2.000	0.097	3.735	0.536	2.721	0.092	3.556	6.149	3.085
2.025	0.108	5.529	0.524	2.423	0.112	5.738	5.510	4.625
			$\mu = 2$		$d = 0.4$			
1.550	0.011	0.895	0.774	0.574	0.008	0.675	12.081	0.843
1.650	0.019	1.379	0.737	0.646	0.014	1.037	11.253	1.017
1.750	0.030	1.935	0.699	0.740	0.023	1.473	10.349	1.205
1.850	0.046	2.575	0.653	0.899	0.036	2.021	9.274	1.598
1.925	0.062	2.842	0.616	1.101	0.051	2.343	8.314	1.841

T	p_s	$\delta p_s 10^4$	ρ'	$10^3\delta\rho'$	ρ''	$10^4\delta\rho''$	Δh_V	$100\delta\Delta h_V$
1.975	0.074	3.663	0.585	1.212	0.063	3.136	7.573	2.491
2.025	0.089	3.743	0.555	1.903	0.082	3.432	6.694	3.492
2.060	0.102	4.271	0.532	2.092	0.101	4.203	5.960	3.768
			$\mu = 2$		$d = 0.5$			
1.575	0.009	0.718	0.779	0.548	0.006	0.535	12.799	0.935
1.650	0.013	0.987	0.754	0.607	0.010	0.732	12.170	0.943
1.725	0.020	1.298	0.729	0.606	0.015	0.971	11.478	1.124
1.800	0.028	1.820	0.699	0.895	0.021	1.372	10.768	1.432
1.875	0.039	2.572	0.669	0.947	0.030	2.003	9.914	1.555
1.925	0.048	2.758	0.647	1.064	0.038	2.197	9.329	1.922
1.975	0.058	2.788	0.618	1.411	0.048	2.284	8.648	2.230
2.025	0.071	3.393	0.592	2.936	0.061	2.927	7.861	3.161
2.075	0.084	3.712	0.554	6.316	0.077	3.408	6.933	5.528
2.110	0.095	4.840	0.537	2.565	0.091	4.676	6.341	4.880
2.160	0.113	4.908	0.500	4.354	0.123	5.338	5.156	6.755
			$\mu = 2.2$		$d = 0.3$			
1.650	0.009	0.748	0.779	0.572	0.006	0.525	13.435	0.986
1.775	0.017	1.094	0.737	0.747	0.012	0.766	12.424	1.141
1.900	0.031	2.299	0.690	0.988	0.022	1.658	11.150	1.609
1.950	0.038	2.123	0.670	1.019	0.028	1.556	10.618	1.836
2.025	0.051	2.836	0.636	1.124	0.039	2.154	9.709	2.050
2.070	0.060	3.328	0.612	1.452	0.047	2.603	9.087	2.252
2.120	0.071	3.493	0.585	1.458	0.057	2.818	8.397	2.917
2.170	0.085	3.951	0.553	2.029	0.074	3.436	7.419	4.631
2.250	0.113	5.493	0.492	4.246	0.116	5.660	5.511	7.763
			$\mu = 2.2$		$d = 0.4$			
1.700	0.009	0.841	0.775	0.644	0.006	0.585	13.739	1.051
1.800	0.015	1.117	0.744	0.594	0.011	0.776	12.905	1.106
1.900	0.024	1.825	0.706	1.013	0.017	1.283	11.931	1.795
2.000	0.037	2.114	0.669	1.020	0.027	1.538	10.842	1.935
2.125	0.060	2.749	0.608	1.540	0.047	2.154	9.173	2.568
2.200	0.079	4.069	0.572	1.927	0.068	3.512	7.877	4.184
2.200	0.078	3.111	0.566	3.520	0.067	2.665	7.862	4.504
2.250	0.091	3.847	0.534	2.203	0.082	3.447	7.034	4.550
2.300	0.110	4.861	0.498	2.355	0.112	4.970	5.725	5.749
			$\mu = 2.2$		$d = 0.5$			
1.800	0.010	0.925	0.758	0.873	0.007	0.634	14.179	1.620
1.875	0.015	1.098	0.736	0.762	0.010	0.764	13.394	1.517
1.950	0.020	1.327	0.709	0.851	0.014	0.924	12.666	1.587
2.025	0.029	1.892	0.683	0.863	0.021	1.358	11.787	1.905
2.100	0.039	2.185	0.651	1.172	0.029	1.611	10.887	2.379

T	p_s	$\delta p_s 10^4$	ρ'	$10^3\delta\rho'$	ρ''	$10^4\delta\rho''$	Δh_V	$100\delta\Delta h_V$
2.175	0.051	2.490	0.617	1.779	0.039	1.914	9.888	2.818
2.225	0.062	3.035	0.595	1.703	0.050	2.460	9.062	3.339
2.275	0.038	3.743	0.568	1.669	0.063	3.208	8.195	4.330
2.350	0.096	4.246	0.520	2.885	0.095	4.188	6.529	5.985
2.400	0.109	5.501	0.468	5.327	0.111	5.596	5.585	9.405
			$\mu = 2.45$		$d = 0.3$			
1.950	0.012	0.879	0.752	0.626	0.008	0.556	14.870	1.271
2.000	0.015	1.107	0.735	0.844	0.010	0.701	14.403	1.502
2.075	0.021	1.353	0.711	0.901	0.013	0.867	13.666	1.671
2.150	0.028	1.557	0.685	0.896	0.019	1.018	12.851	2.054
2.225	0.039	2.146	0.658	1.034	0.026	1.465	11.865	2.289
2.300	0.050	2.461	0.627	1.168	0.035	1.746	10.918	2.645
2.350	0.060	2.909	0.602	1.462	0.045	2.167	10.062	3.254
2.400	0.072	3.584	0.581	1.812	0.057	2.857	9.160	4.493
2.450	0.081	3.190	0.543	2.153	0.065	2.553	8.491	4.111
2.500	0.096	4.105	0.509	3.599	0.084	3.598	7.303	7.053
2.550	0.113	5.445	0.473	3.422	0.111	5.387	5.949	8.419
			$\mu = 2.45$		$d = 0.4$			
2.025	0.012	1.053	0.742	0.819	0.008	0.668	15.040	1.862
2.075	0.015	1.337	0.726	0.968	0.010	0.850	14.589	2.131
2.200	0.026	1.934	0.683	1.128	0.017	1.267	13.206	2.184
2.300	0.039	1.867	0.646	1.281	0.027	1.288	11.901	3.113
2.400	0.054	2.670	0.600	1.704	0.039	1.953	10.506	3.939
2.465	0.068	3.159	0.569	2.254	0.053	2.480	9.338	3.859
2.525	0.082	3.309	0.539	3.379	0.069	2.790	8.243	5.384
2.550	0.090	4.899	0.529	2.687	0.084	4.569	7.399	7.185
2.575	0.095	4.435	0.502	2.283	0.087	4.037	7.145	7.191
2.600	0.103	5.320	0.489	2.826	0.097	5.021	6.675	8.033
			$\mu = 2.45$		$d = 0.5$			
2.250	0.019	1.294	0.689	1.058	0.013	0.855	14.319	2.984
2.300	0.023	1.547	0.670	1.125	0.016	1.034	13.716	3.064
2.350	0.029	1.655	0.656	1.323	0.020	1.135	13.045	3.407
2.400	0.035	1.997	0.637	1.680	0.025	1.415	12.287	3.498
2.450	0.042	2.389	0.617	1.765	0.030	1.746	11.550	3.932
2.500	0.048	2.328	0.592	1.771	0.035	1.699	11.047	3.968
2.550	0.059	2.716	0.575	1.786	0.047	2.192	9.833	5.011
2.600	0.070	3.609	0.544	2.329	0.060	3.110	8.775	5.391
2.650	0.080	4.222	0.514	3.286	0.070	3.693	8.128	6.767
2.700	0.098	4.505	0.491	3.684	0.108	5.001	6.139	8.832
2.725	0.105	4.745	0.472	3.580	0.124	5.650	5.493	9.395

Table 3: Critical temperatures T_c of different beak fluids. The uncertainty is about ± 0.01.

μ \ d	0.1	0.2	0.3	0.4	0.5
1.6	1.71	1.74	1.77	1.80	1.83
1.8	1.88	1.91	1.95	1.98	2.02
2	2.06	2.10	2.14	2.18	2.23
2.2	2.26	2.31	2.36	2.41	2.46
2.45	2.54	2.60	2.66	2.72	2.78

Table 4: Fractions of molecules with 0, 1, 2, and 3 H-bonds for different combinations of the reduced dipole moment and charge separation at a temperature of 0.7 T_c. Statistical uncertainties are indicated with a δ.

d	f_0	$10^3 \delta f_0$	f_1	$10^4 \delta f_1$	$10^2 f_2$	$10^4 \delta f_2$	$10^3 f_3$	$10^5 \delta f_3$
				$\mu = 1.6$				
0.10	0.96	0.32	0.04	3.07	0.10	0.25	0.00	0.06
0.20	0.62	1.05	0.33	8.27	5.10	3.97	2.00	5.18
0.30	0.34	1.20	0.46	7.11	17.80	8.71	18.00	23.54
0.40	0.25	1.06	0.47	6.91	24.70	9.08	30.00	29.34
0.50	0.20	1.00	0.46	6.74	30.30	10.00	38.00	34.15
				$\mu = 2$				
0.10	0.90	0.53	0.10	5.13	0.30	0.61	0.00	0.35
0.20	0.51	1.11	0.40	8.86	9.10	4.93	4.00	8.98
0.30	0.26	1.08	0.47	7.29	24.30	9.51	25.00	33.10
0.40	0.17	0.82	0.46	8.42	33.50	10.80	40.00	34.05
0.50	0.10	0.72	0.41	9.93	44.00	12.70	53.00	37.42
				$\mu = 2.45$				
0.10	0.79	0.68	0.20	5.92	1.40	1.65	0.00	0.84
0.20	0.38	1.17	0.46	8.19	15.40	8.15	8.00	13.12
0.30	0.17	0.81	0.46	7.64	33.50	10.40	34.00	28.87
0.40	0.09	0.66	0.40	9.50	46.10	11.60	50.00	37.69
0.50	0.04	0.49	0.28	10.30	63.20	13.90	54.00	44.79

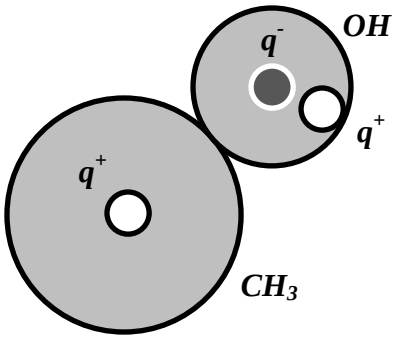

Figure 1: Methanol model of Schnabel *et al.*[10] comprising a CH_3 group, modeled as a single LJ-site and an OH group modeled as a LJ-site with three point charges placed properly on the molecular model.

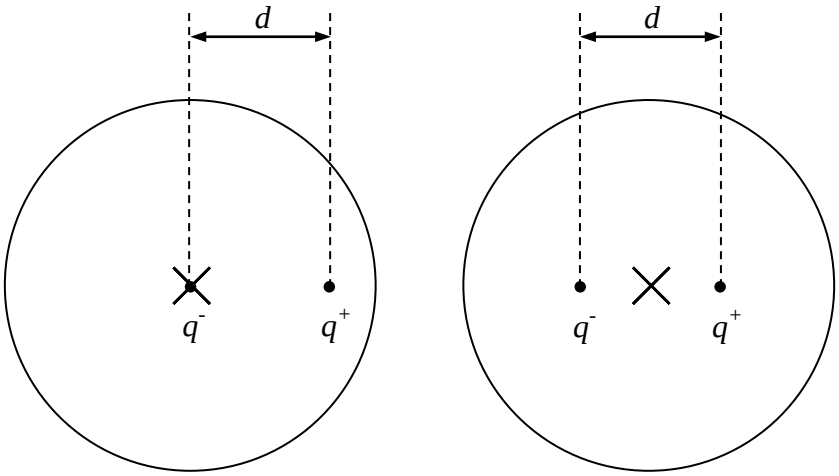

Figure 2: Beak (left) and symmetric (right) model studied in the present work. The crosses mark the position of Lennard-Jones sites and the bullets represent point charges.

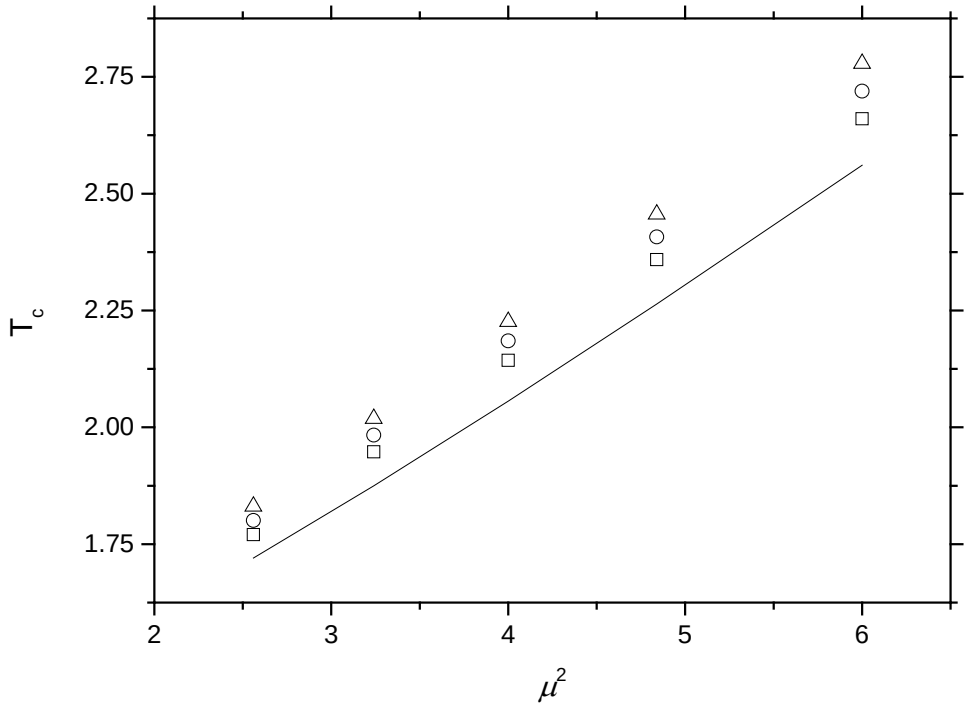

Figure 3: Critical temperature T_c of the beak fluid as a function of μ^2 and d, where the dependence on d is indicated by isolines for d equal to 0.3 (squares), 0.4 (circles) and 0.5 (triangles). The lowest line shows the critical points[18] of the Stockmayer fluid for comparison.

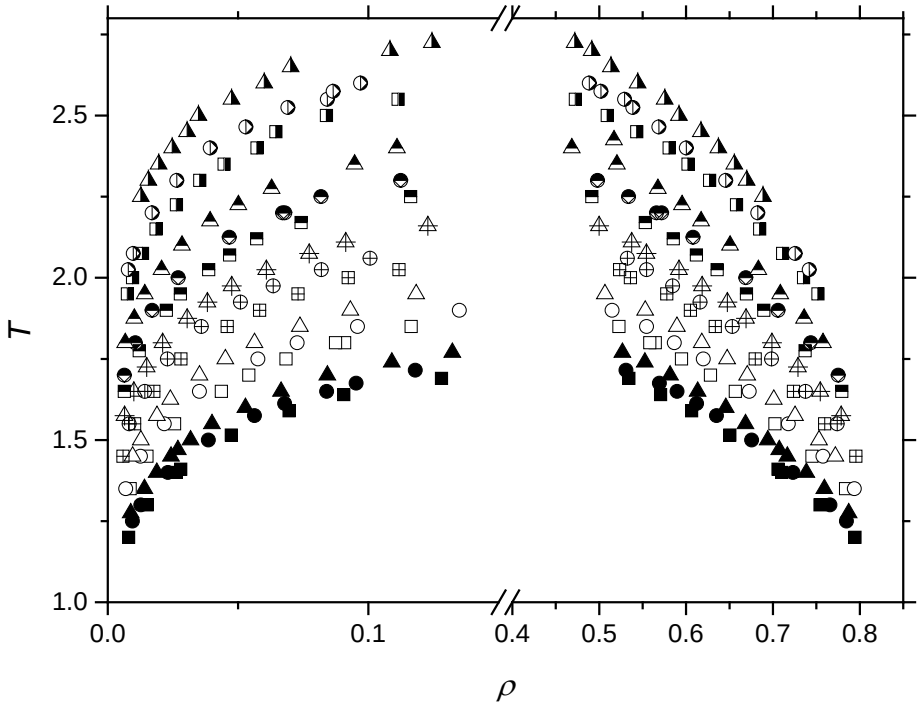

Figure 4: Vapor-liquid equilibrium of different beak fluids. See Table 1 for specifications and assignment of symbols.

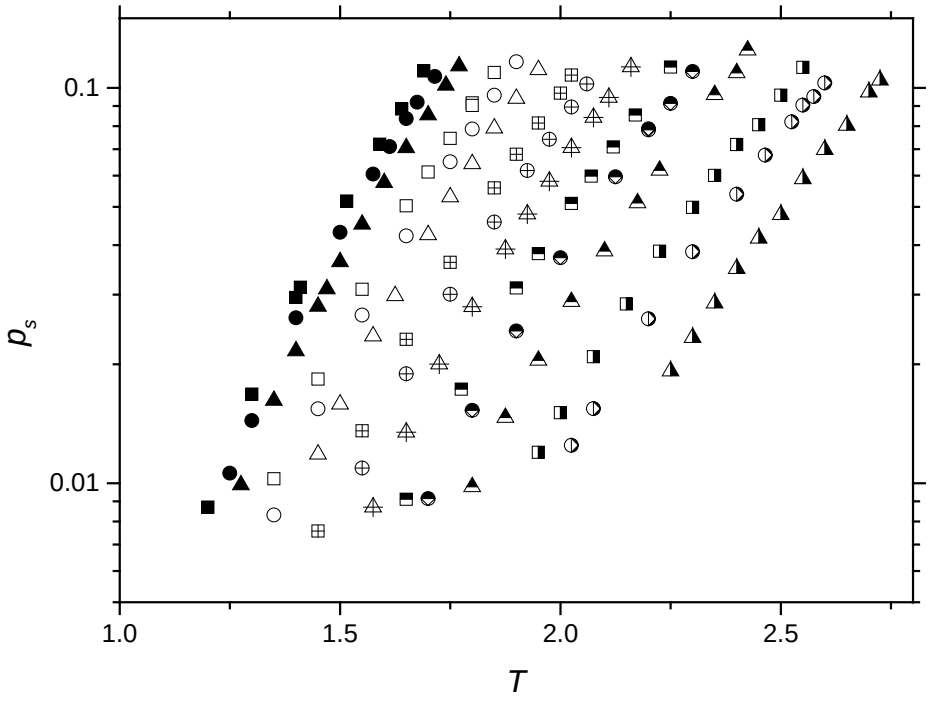

Figure 5: Vapor pressure curves of different beak fluids. See Table 1 for specifications and assignment of symbols.

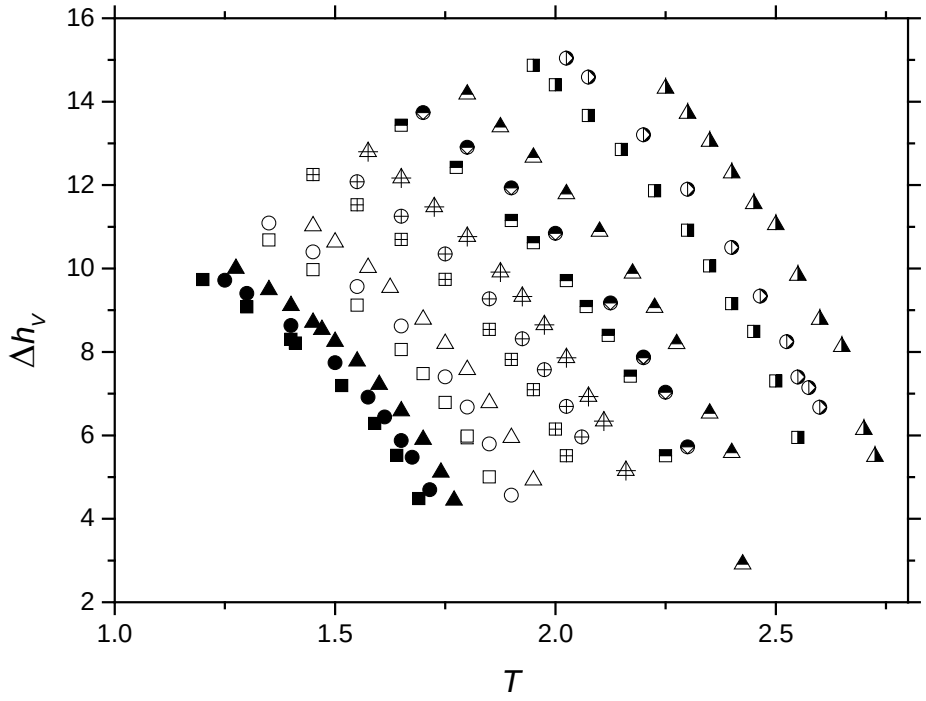

Figure 6: Enthalpy of vaporization of different beak fluids. See Table 1 for specifications and assignment of symbols

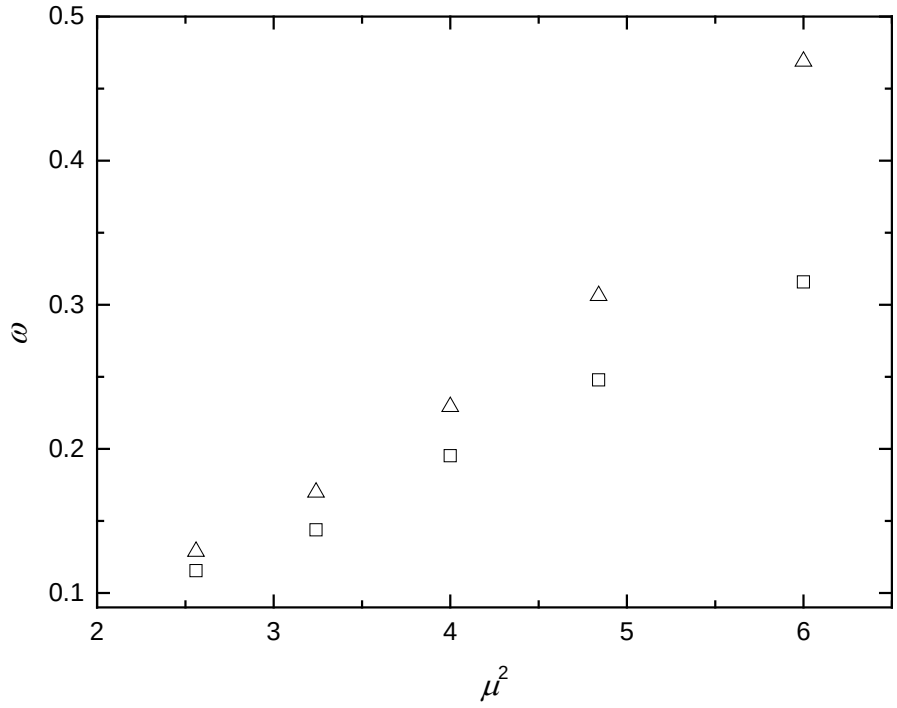

Figure 7: Acentric factor ω of the beak fluid as a function of μ^2 and *d*, where the dependence on *d* is indicated by isolines for *d* equal to 0.3 (squares) and 0.5 (triangles).

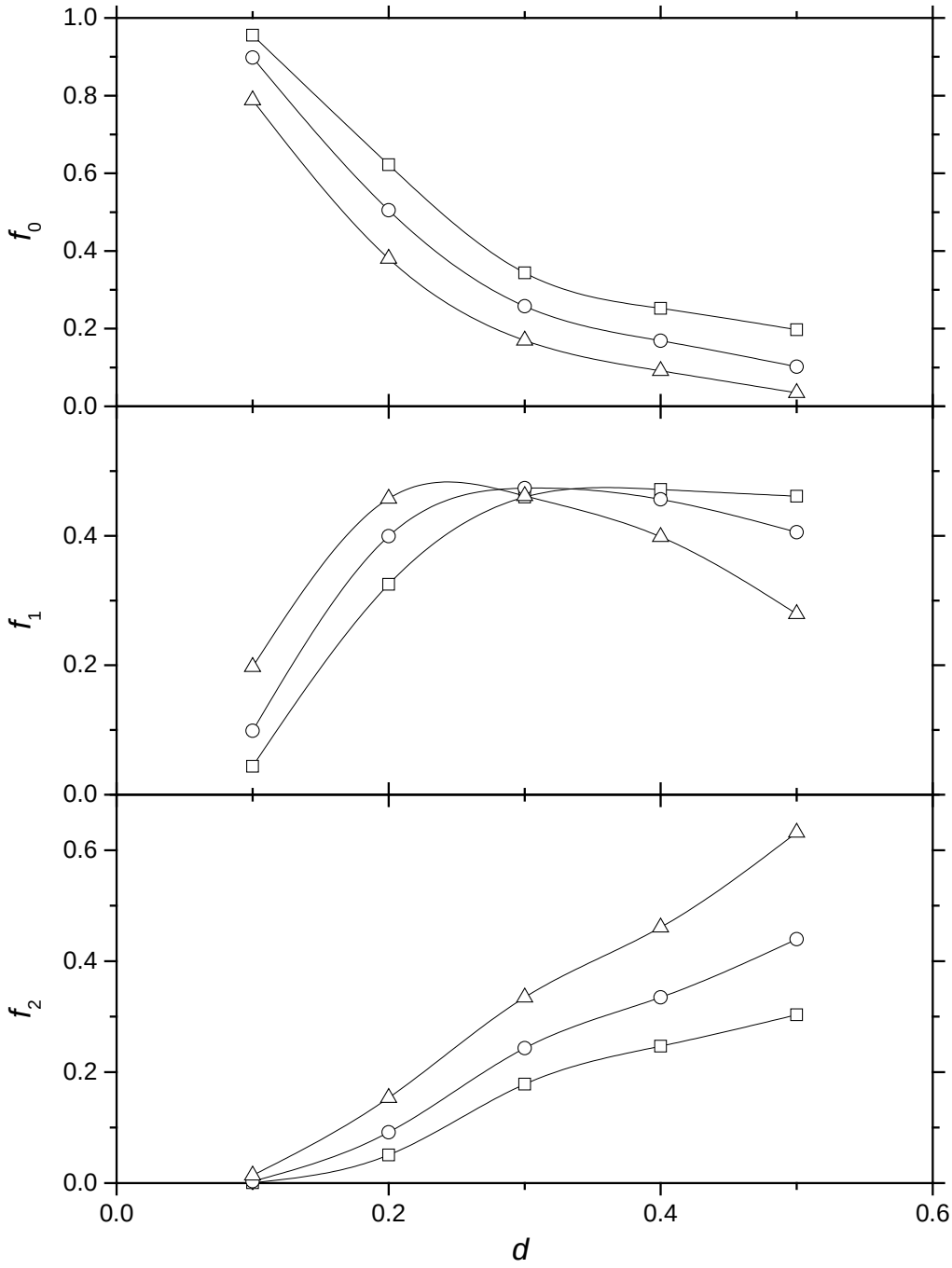

Figure 8: Fractions f_i of molecules with i = 0, 1 and 2 H-bonds for the beak model at 0.7 the critical temperature over the reduced charge separations for three dipole moments μ equal to 1.6 (squares), 2 (circles) and 2.45 (triangles).

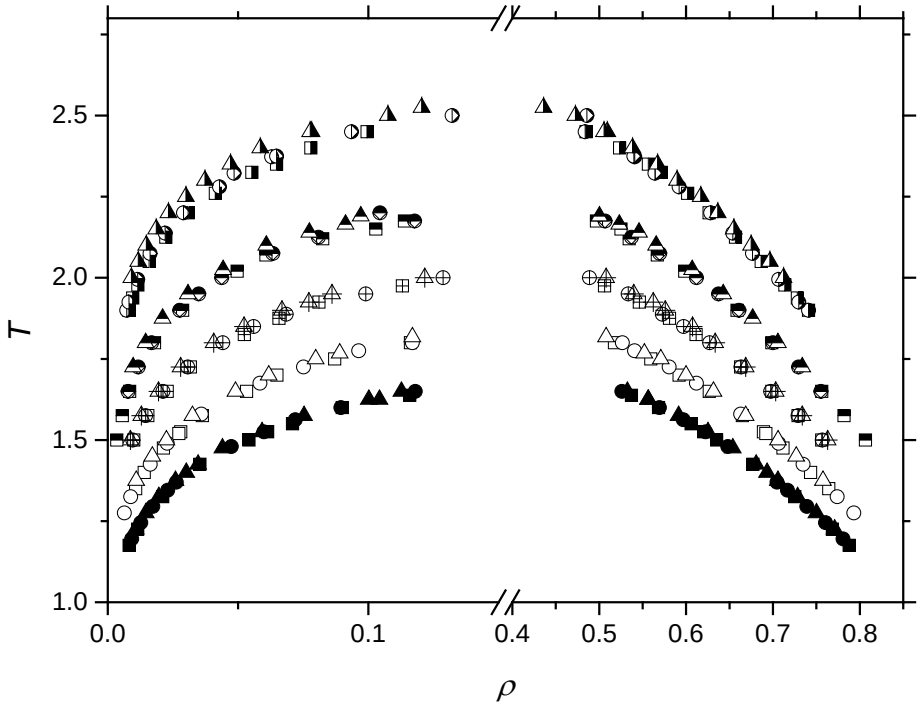

Figure 9: Vapor-liquid equilibrium determined for different symmetric models, see Table 1 for specifications and assignment of symbols.